

Spatial variability enhances species fitness in stochastic predator–prey interactions

Ulrich Dobramysl^{1,*} and Uwe C. Täuber^{2,†}

¹*Institute of Semiconductor and Solid State Physics,
Johannes Kepler University, Altenbergerstr. 69, 4040 Linz, Austria*

²*Department of Physics, Virginia Tech, Blacksburg, VA 24061-0435*
(Dated: November 11, 2018)

We study the influence of spatially varying reaction rates on a spatial stochastic two-species Lotka–Volterra lattice model for predator–prey interactions using two-dimensional Monte Carlo simulations. The effects of this quenched randomness on population densities, transient oscillations, spatial correlations, and invasion fronts are investigated. We find that spatial variability in the predation rate results in more localized activity patches, which in turn causes a remarkable increase in the asymptotic population densities of both predators and prey, and accelerated front propagation.

PACS numbers: 87.23.Cc, 87.18.Tt, 05.40.-a

Understanding biological diversity has been a central issue in ecology [1, 2, 3, 4]. In order to understand the coexistence of competing species, several simplified ‘toy’ models for the dynamics of few interacting populations such as the paradigmatic Lotka–Volterra predator–prey model have been investigated. More recently, the crucial role of spatial fluctuations and stochasticity in stabilizing such systems has been recognized [5]. Indeed, stochastic predator–prey models [6, 7, 8] that consistently account for the internal reaction noise yet reduce to the classical coupled Lotka–Volterra differential equations in the well-mixed mean-field limit have been found to display a remarkable wealth of intriguing features [9]: In contrast to the regular nonlinear oscillations of the deterministic Lotka–Volterra model which always entail a return to the initial state, these stochastic spatial models yield long-lived, but ultimately decaying erratic population oscillations [10, 11, 12, 13, 14, 15]. In the absence of spatial degrees of freedom, these oscillations can be understood through a resonant amplification mechanism for stochastic fluctuations that drastically extends the transient period before the (finite) system finally reaches the absorbing stationary state (predator extinction) [16]. In spatially extended systems, the mean-field Lotka–Volterra reaction-diffusion model is known to support traveling wave solutions [17, 18, 19]. In corresponding stochastic spatial population models, spreading activity fronts induce persistent correlations between the prey and predator species, and further enhance the amplitude and life time of local population oscillations [9, 20, 21].

In our studies of different stochastic spatial model variants for competing predator–prey populations, we have found these intriguing spatio-temporal structures and the overall features to be remarkably generic and robust with respect to even rather drastic changes of the detailed microscopic interaction rules [20, 22]. Yet to render these models more realistic and relevant for biological systems, one must obviously allow for different fitness of the individuals as well as spatial variations in the rates that describe the population kinetics. In this letter, we ad-

dress the latter situation by considering the reaction rates to be quenched random variables, drawn from truncated Gaussian distributions. This model can be interpreted as describing a direct environmental influence on the species death and reproduction rates such as, e.g., a local variability of available resources.

By means of individual-based stochastic cellular automaton Monte Carlo simulations we find that an increasing spatial variation of the predation interaction or species invasion rate (with fixed mean) enhances the steady-state population densities (which we take as a measure of the species’ fitness) of *both* predators and prey. In contrast, mere variations of the predator death and prey reproduction rates have very little effect. While a simple mean-field averaging over varying predation rates does indeed predict a marked stationary density increase, it also grossly overestimates cooperative behavior and cannot adequately describe our numerical results. In fact, we shall argue that the principal fitness enhancement mechanism rests in the fact that stronger disorder in the predation rate reduces the size of the localized regions populated by both species, thus amplifying the initial local population oscillations and permitting a larger number of activity patches in the asymptotic long-time limit. Thus, the fitness enhancement of both species through spatial variability, notably in the absence of any evolutionary adaption processes, is a consequence of the emerging dynamical correlations. Remarkably, we find that quenched randomness in the predation rates also slightly increases the speed of spreading activity fronts.

We consider a stochastic Lotka–Volterra model on a square lattice (typically with 512×512 sites) with periodic boundary conditions. Individuals of both particle species perform random walks through unbiased nearest-neighbor hopping (which occurs with probability one, so in effect all rates listed below are to be understood as relative to the diffusivity D). We allow multiple, essentially unrestricted lattice site occupation for particles of either or both species (the maximum number per site i is capped at $n_i \leq 1000$). This eliminates the predator

extinction transition present in model variants with restricted site occupation [9, 14, 20]. The ‘predator’ species is subject to spontaneous decay $A \rightarrow \emptyset$ with rate μ , in contrast with the ‘prey’ particles that may produce offspring $B \rightarrow 2B$ with rate σ . When individuals of both species meet on any lattice site, a prey is ‘eaten’ and the predators simultaneously reproduce, i.e., we implement the predation interaction $A + B \rightarrow 2A$ with rate λ . Our dynamical Monte Carlo simulation proceeds with random sequential updates; a Monte Carlo step (MCS) is completed once on average each particle in the system has been moved and had the chance to react [23].

Spatial variability is introduced by drawing the reaction probabilities for each lattice site from normalized Gaussian distributions, truncated at the values 0 and 1, with fixed mean (in most cases $\bar{\mu} = \bar{\sigma} = \bar{\lambda} = 0.5$) but different standard deviations $\sigma = 0 \dots 0.9$. The reaction rates therefore constitute quenched random variables.

The time evolution of the mean predator density $\rho_A(t) = \langle n_{Ai}(t) \rangle$, averaged over 50 Monte Carlo simulation runs with initially randomly placed particles with densities $\rho_A(0) = \rho_B(0) = 1$ is shown in Fig. 1(a). The absolute value of the Fourier transform (taken over the full interval of 500 Monte Carlo steps) of this averaged signal, $|\rho_A(\omega)|$, is displayed in Fig. 1(b). Here we have used uniform rates $\mu = \sigma = 0.5$, while the predation rate represents a quenched random variable with mean $\bar{\lambda} = 0.5$ and standard deviation σ_λ ranging from 0 to 0.9 [26]. For these rates, the prey population density (not shown) behaves similarly, with an overall phase shift in the transient oscillations [24], and both densities reach practically identical asymptotic density values, see also Fig. 2(a). It is evident that increasing spatial variability markedly amplifies the initial population oscillations and reduces the relaxation time towards the steady state. Remarkably, *both* predator and prey densities approach larger asymptotic values as σ_λ is raised. As shown in Fig. 2(a), either species gains a remarkable fitness enhancement by $\sim 25\%$ in the investigated σ_λ range. We have also studied spatial variations in the predator death rate μ and the prey birth rate σ , with the other rates held uniform. In either case we observe merely a minute increase in the few percent range of the asymptotic predator and prey densities, not nearly as pronounced as the effect of spatially varying predation rates.

The neutrally stable species coexistence fixed point of the classical Lotka–Volterra mean-field rate equations gives the stationary predator and prey densities as $\rho_A = \sigma/\lambda$ and $\rho_B = \mu/\lambda$. Presumably therefore, the fitness enhancement of both species stems from those regions where the predation rate is significantly lower than the average. Before we explore local effects in more detail, let us first consider a global average over the truncated Gaussian predation rate distributions of these mean-field stationary densities. The result is depicted in Fig. 2(a) along with the simulation data: The ‘naive’ averaging

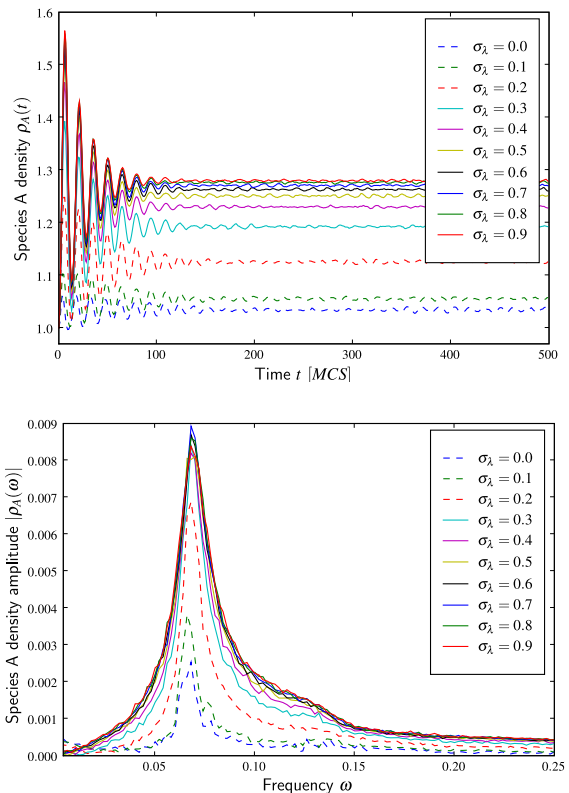


FIG. 1: (a) Time evolution of the predator density $\rho_A(t)$, averaged over 50 Monte Carlo simulation runs on a 512×512 square lattice with initial densities $\rho_A(0) = \rho_B(0) = 1$, predator death rate $\bar{\mu} = 0.5$, prey birth rate $\bar{\sigma} = 0.5$, and mean predation rate $\bar{\lambda} = 0.5$, for different variances σ_λ as indicated. (b) Signal Fourier transform $|\rho_A(\omega)|$. (Color online.)

procedure indeed yields an increase of both stationary population densities; however, it predicts a grossly exaggerated fitness enhancement owing to the fact that mean-field approximations tend to overestimate cooperative effects [25]. We therefore proceed to investigate the prominent role of spatial variations and predator–prey correlations in the lattice system.

As one would expect, increasing disorder broadens the peak associated with the transient oscillations in the associated Fourier signal, reflecting faster relaxation towards the asymptotic nonequilibrium stationary state. Figure 1(b) clearly reveals the roughly threefold increase in amplitude of the stochastic nonlinear population oscillations as σ_λ is raised from 0 to 0.9. By fitting the peak envelopes to a Lorentzian shape (which works well except in the pure case with $\sigma_\lambda = 0$), we extracted the characteristic relaxation times $\tau_{\text{relax } A/B} = 1/\Gamma_{A/B}$ from the full widths at half maximum $\Gamma_{A/B}$ as function of σ_λ , see Fig. 2(b). Note the reduction by a factor ~ 2.5 in $\tau_{\text{relax } A/B}$ as σ_λ is increased from 0.1 to 0.6.

The increasing amplitudes of the initial population oscillations suggest that the spatial variability in the predation rates tends to cluster both species closer to-

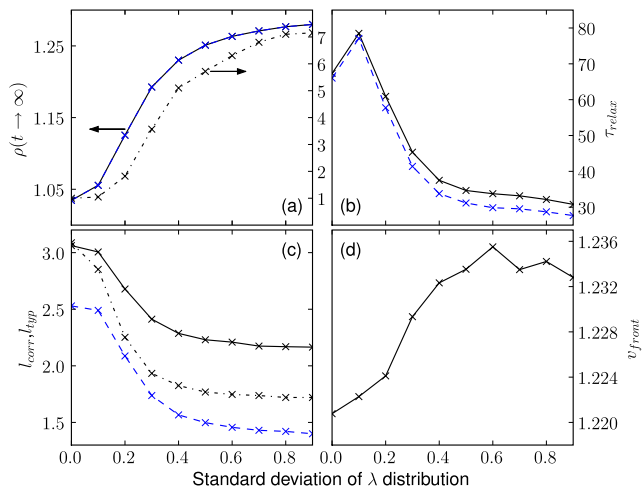


FIG. 2: Dependence on the variance σ_λ , measured for uniform rates $\mu = \sigma = 0.5$ of (a) the asymptotic mean population densities $\rho_{A/B}(t \rightarrow \infty)$, compared with the average over the mean-field values (dashed-dotted lines, right-hand y-axis), (b) the relaxation time $\tau_{\text{relax } A/B}$ towards the stationary state, (c) the predator/prey correlation lengths $l_{\text{corr } A/B}$ – predators A : full lines, prey B : dashed – and the typical species separation distance l_{typ} : dashed-dotted line; (d) the front speed v_{front} of the activity rings, obtained for $\mu = 0.2$ and $\sigma = 1.0$.

gether, thus enhancing localized population explosions. This interpretation is in fact borne out by measuring the steady-state equal-time two-point correlation functions $C_{\alpha\beta}(x) = \langle n_{\alpha i+x} n_{\beta i} \rangle - \rho_\alpha \rho_\beta$ with $\alpha, \beta = A, B$ [27]. After again averaging the data over 50 Monte Carlo simulation runs, we have extracted the predator and prey correlation lengths $l_{\text{corr } A/B}$, which essentially measure the spatial extent of the population patches, as function of σ_λ by least-square fits of $C_{AA}(x)$ and $C_{BB}(x)$ to exponentials $\exp(-|x|/l_{\text{corr}})$ at sufficiently large distance $|x|$. As depicted in Fig. 2(c), the predator correlation length $l_{\text{corr } A}$ decreases by $\sim 30\%$ from about 3 to 2.1 lattice constants as the disorder variance increases, while $l_{\text{corr } B}$ is reduced by $\sim 45\%$ from 2.5 to 1.4.

Similarly, we infer the typical predator–prey separation distance l_{typ} from the cross-correlation function $C_{AB}(x)$, which is negative at short distances, but attains a maximum with positive correlation before tending towards 0 as $|x| \rightarrow \infty$ [27]. Here, we define l_{typ} as the location of the maximum of $C_{AB}(x)$. The results as function of the standard deviation σ_λ , shown in Fig. 2(c), closely follow the behavior of the correlation lengths, namely rather rapidly decreasing from ~ 3 lattice constants to ~ 1.7 as σ_λ is reduced from 0.1 to 0.4. Thus, when the width of the distribution of the spatially varying predation rates λ becomes larger, the ensuing correlated patches of coexisting predator–prey populations become more localized in regions with low values of λ . Consequently, a larger number of such patches can be accommodated in the system, whereby the long-time population densities increase. The

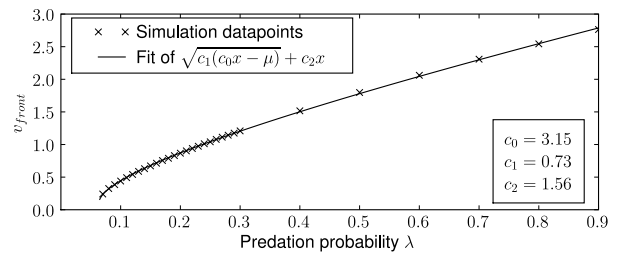


FIG. 3: Propagation speed of radially spreading activity fronts in the stochastic Lotka–Volterra model with uniform rates $\mu = 0.2$ and $\sigma = 0$ as function of the predation rate λ . The square-root fit is inspired by the mean–field lower bound.

stabilizing effect of spatial inhomogeneity has recently been elaborated in a two-patch predator–prey model of diffusively coupled two-dimensional oscillators [28].

The classical two-species Lotka–Volterra reaction–diffusion equations, i.e., essentially the mean-field rate equations supplemented with diffusive spreading, are well-known to support traveling wave solutions [4, 17, 18, 19], whose minimal front speed can be established by standard mathematical tools [29, 30, 31]. Beyond the mean-field approximation, however, already in single-species systems the incorporation of intrinsic reaction noise in the computation of wave front propagation velocities is a rather difficult problem [32, 33, 34, 35, 36], and there are very few results available for two-species models [35, 37].

In the initial stage of our simulations, we observe radially spreading circular fronts of prey followed by predators [26]. We have therefore set out to numerically measure the front propagation speed of spreading rings of activity, namely prey invading empty regions followed by predators feeding on them, in our two-dimensional stochastic Lotka–Volterra model. To this end, we set up as initial state a circular patch of B particles, one per site, of radius 5 lattice constants, and 10 predators A located on the center site of this patch. In this study, we have chosen uniform rates $\mu = 0.2$ and $\sigma = 1.0$, with spatially varying predation rate with mean $\bar{\lambda} = 0.5$. After angular averaging to obtain the radial particle concentrations, we have determined the invading front location by searching for the zero of the first derivative of the radial prey density. A linear fit of the data with Monte Carlo time yields the front speed v_{front} , which is then averaged over typically 50 simulation runs. The change of propagation speed with the disorder variance σ_λ is plotted in Fig. 2(d). We find a small but noticeable $\sim 1\%$ increase of the spreading activity front speed as σ_λ is raised from 0 to 0.7, which we interpret as essentially a consequence of the larger amplitudes of the more localized population fluctuations caused by the spatial variability of the predation rate. Our results for spatially homogeneous rates are depicted as function of the predation rate in Fig. 3. To avoid problems at small λ values due to prey population explosions, we chose as initial state a sea of

unreproductive B particles (5 per site) and 5 predators A located on the center of the grid, with $\mu = 0.2$. The data can be fitted reasonably well with a square-root expression that is motivated by the known lower bound $v_{front} > \sqrt{4D_A(\lambda'\rho - \mu)}$, where ρ denotes the prey carrying capacity [4, 17, 18]. Here, $4D_A = 1$, $\rho = 1000$, but the dimensionless reaction probability $\lambda'\rho \sim \lambda$, so indeed the fit constants c_0 and c_1 should be of order 1, but capture fluctuation-induced renormalizations of the mean-field parameters, and the additional offset $c_2 > 0$ describes the deviation from the lower bound.

In conclusion, we have employed Monte Carlo simulations to investigate a stochastic two-species Lotka–Volterra model subject to quenched disorder in the reaction rates on a two-dimensional lattice without occupation number restrictions. While randomizing the prey birth and predator death rates has little effect, spatial variability in the predation / species invasion rate λ markedly enhances the asymptotic densities for both predator and prey populations. We provide evidence that this remarkable fitness increase is caused by disorder-induced modifications in the emerging spatio-temporal structures: Upon increasing the width of the random rate distribution, the typical length scales of both the spatial predator–predator and the prey–prey correlations is reduced. This results in more localized patches of activity, presumably in the vicinity of regions where the local predation rates are smaller than their mean value. The system is thus able to accommodate a larger amount of populated regions. We also find that spatial variability in the predation rate drastically amplifies the initial population oscillations and markedly reduces the time required to reach the steady-state configuration. In contrast, the front speed of spreading activity rings from a localized center is not very strongly affected by the disorder. Yet we do observe that the activity fronts accelerate slightly upon increasing the variance of the predation rate.

This research has been supported in part through the IAESTE International Student Exchange Program and the U.S. National Science Foundation, grant nsf-dmr 0308548. We gratefully acknowledge inspiring discussions with J. Banavar, R. Kulkarni, M. Mobilia, M. Pleimling, B. Schmittmann, N. Shnerb, and R. K. P. Zia.

* Electronic address: ulrich.dobramysl@jku.at

† Electronic address: tauber@vt.edu

- [1] R. M. May, *Stability and complexity in model ecosystems*, (Princeton University Press, Princeton, 1973).
- [2] J. Maynard Smith, *Models in ecology* (Cambridge University Press, Cambridge, 1974).
- [3] J. Hofbauer and K. Sigmund, *Evolutionary games and population dynamics* (Cambridge University Press, Cambridge, 1998).
- [4] J. D. Murray, *Mathematical biology*, Vols. I and II (Springer, New York, 3rd ed. 2002).
- [5] R. Durrett, *SIAM Review* **41**, 677 (1999).
- [6] H. Matsuda, N. Ogita, A. Sasaki, and K. Satō, *Prog. Theor. Phys.* **88** 1035 (1998).
- [7] J. E. Satulovsky and T. Tomé, *Phys. Rev. E* **49**, 5073 (1994).
- [8] N. Boccara, O. Roblin, and M. Roger, *Phys. Rev. E* **50**, 4531 (1994).
- [9] For a recent overview, see M. Mobilia, I. T. Georgiev, and U. C. Täuber, *J. Stat. Phys.* **128**, 447 (2007).
- [10] A. Provata, G. Nicolis, and F. Baras, *J. Chem. Phys.* **110**, 8361 (1999).
- [11] A. F. Rozenfeld and E. V. Albano, *Physica A* **266**, 322 (1999).
- [12] A. Lipowski, *Phys. Rev. E* **60**, 5179 (1999).
- [13] M. Droz and A. Pękaliski, *Phys. Rev. E* **63**, 051909 (2001).
- [14] T. Antal and M. Droz, *Phys. Rev. E* **63**, 056119 (2001).
- [15] M. Kowalik, A. Lipowski, and A. L. Ferreira, *Phys. Rev. E* **66**, 066107 (2002).
- [16] A. J. McKane and T. J. Newman, *Phys. Rev. Lett.* **94**, 218102 (2005).
- [17] S. R. Dunbar, *J. Math. Biol.* **17**, 11 (1983).
- [18] J. Sherratt, B. T. Eagen, and M. A. Lewis, *Phil. Trans. R. Soc. Lond. B* **352**, 21 (1997).
- [19] M. A. M. de Aguiar, E. M. Rauch, and Y. Bar-Yam, *J. Stat. Phys.* **114**, 1417 (2004).
- [20] M. J. Washenberger, M. Mobilia, and U. C. Täuber, *J. Phys. Condens. Matter* **19**, 065139 (2007).
- [21] The oscillation amplitudes for the global population densities decrease with system size and vanish in the thermodynamic limit, as a consequence of averaging over out-of-phase oscillations; see, e.g., Fig. 7 in Ref. [9].
- [22] M. Mobilia, I.T. Georgiev, and U.C. Täuber, *Phys. Rev. E* **73**, 040903(R) (2006).
- [23] Additional details of the Monte Carlo simulation algorithm are described in Ref. [20].
- [24] These oscillations persist much longer in single simulation runs, see Fig. 7 in Ref. [9] and Fig. 5 in Ref. [20].
- [25] We note that this mean-field average is sensitive to the cutoff at small values of λ . This is obvious in the flat distribution limit $\sigma_\lambda \rightarrow \infty$, which yields a logarithmic dependence on the integration boundaries.
- [26] Two sets of simulation movies are accessible at <http://www.phys.vt.edu/~tauber/PredatorPrey/movies/>:
(i) uniform $\mu = 0.5$, $\sigma = 0.2$, $\bar{\lambda} = 0.5$, $\sigma_\lambda = 0$ and 0.5;
(ii) $\mu = 0.5$, $\sigma = 0.5$, $\bar{\lambda} = 0.5$, $\sigma_\lambda = 0, 0.3$, and 0.5.
- [27] For stochastic Lotka–Volterra models with spatially uniform rates, these correlation functions are depicted in Figs. 4–6 of Ref. [9] and Fig. 5 in Ref. [20].
- [28] G. Yaari, S. Solomon, M. Schiffer, and N.M. Shnerb, Preprint (2008).
- [29] Y. Hosono, *Bull. Math. Biol.* **60**, 435 (1998).
- [30] V. Méndez, J. Fort, and J. Farjas, *Phys. Rev. E* **60**, 5231 (1999).
- [31] M. A. Lewis, B. Li, and H. F. Weinberger, *J. Math. Biol.* **45**, 219 (2002).
- [32] J. Riordan, C. R. Doering, and D. ben-Avraham, *Phys. Rev. Lett.* **75**, 565 (1995).
- [33] A. Lemarchand, A. Lesne, and M. Mareschal, *Phys. Rev. E* **51**, 4457 (1995).
- [34] L. Pechenik and H. Levine, *Phys. Rev. E* **59**, 3893 (1999).
- [35] D. Panja, *Phys. Rep.* **393**, 87 (2004).

[36] C. Escudero, Phys. Rev. E **70**, 041102 (2004).

[37] L. O'Malley, B. Kozma, G. Korniss, Z. Rácz, and T.

Caraco, Phys. Rev. E **74**, 041116 (2006).